Kinetic Analysis of the Effects of Mutagenesis of W501 and V432 of the Hepatitis C Virus NS3 Helicase Domain on ATPase and Strand-Separating Activity

Frank Preugschat,* Dana P. Danger, Luke H. Carter, III, Roderick G. Davis, and David J. T. Porter

Glaxo Wellcome, 5 Moore Drive, Research Triangle Park, North Carolina 27709

Received October 13, 1999; Revised Manuscript Received January 6, 2000

ABSTRACT: Two hydrophobic residues, W501 and V432, in the nucleic acid (NA) binding pocket of the HCV helicase domain (E) were mutagenized in an effort to investigate contributions of these residues to substrate affinities and to enzymatic activities. The affinities of wild-type [hE(wt)] and mutant enzymes [hE(W501F), hE(W501A), and hE(V432A)] for NA and ATP were determined by monitoring changes in the intrinsic protein fluorescence, in the fluorescence of fluorescently tagged nucleic acid, and in the enzymatic activity. The steady-state kinetic parameters of the mutant enzymes for ATP hydrolysis (at saturating concentrations of NA) were similar to those of hE(wt). hE(W501F), hE(W501A), and hE(V432A) had strand-separating activities that were 136%, 3.8%, and 3.1% of that of hE(wt). The processivities of hE(W501F), hE(W501A), and hE(V432A) were reduced relative to that of hE(wt). The reduced processivities of hE(W501F) and hE(W501A) were primarily due to an increase in the rate of dissociation of E·ATP from E·ATP·NA. The reduced processivity of hE(V432A) was primarily due to a reduction in the intrinsic forward rate constant for strand separation. This result suggested that V432 may constitute part of the forward "stepping" motor of E. hE(W501A) and hE(V432A) did not display a dominant negative phenotype in a steady-state helicase assay with hE(wt). hE(wt) stored in the presence of β-mercaptoethanol was covalently modified at three cysteinyl residues. The biological significance of the potential reactivity of these cysteinyl residues on hE(wt) is unknown.

Helicases are ubiquitous enzymes that catalyze the conversion of double-stranded nucleic acid (dsNA) to single-stranded NA (ssNA), with the concomitant hydrolysis of ATP (*1*). Structural studies have identified two distinct classes of helicases (monomers and hexamers) within the asymmetric units of crystals or electron micrographs (*2*−*5*). Hexameric and monomeric helicases perform the same essential function of strand separation, but are biochemically and genetically distinct (*5*−*8*). Although several models have been proposed, the mechanism by which ATP hydrolysis is coupled to helicase activity is unknown (*9*).

We and others have initiated studies to determine the kinetic and chemical mechanism of how ATP hydrolysis is coupled to helicase activity in a simple monomeric enzyme (*9*). Because of the urgent medical need for the development of an effective antiviral agent against hepatitis C virus (HCV)[1,2] infection, we have chosen to study the HCV NS3 helicase domain (E). The NS3 protein of HCV has at least two enzymatic activities that are necessary for viral replication. The N-terminal 20 kDa domain of NS3 is a serine proteinase domain that is the target of intensive antiviral drug development (*10*, *11*). The C-terminal 50 kDa domain of NS3 is a NA-stimulated NTPase (*12*) and a NTP-dependent helicase (*13*).

Pre-steady-state kinetic studies of the HCV helicase domain show that upon binding of ATP, the enzyme undergoes a conformational change that results in a 95% decrease in the association rate constant for NA. The affinity for NA decreases concomitantly. The enzyme is a NA-stimulated NTPase that exhibits little selectivity for the polynucleotide or NTP used in the hydrolysis reaction. ATP or NA binds to E randomly, and when binding occurs, the basal rate of ATP hydrolysis is stimulated up to 30-fold. The catalytic efficiency of E (with respect to ATP hydrolysis) does not change upon binding of NA; i.e., the increase in k_{cat} for ATP hydrolysis is offset by an increase in the K_m for ATP (*14*). Inhibition studies with NaF, Mg^{2+}, and poly[r(U)] demonstrated that there are two ATP binding sites per monomeric enzyme, but the relationship between site occupancy and enzymatic activity is as yet undefined (*15*).

* To whom correspondence should be addressed. Telephone: (919) 483-9423. Fax: (919) 483-3895. E-mail: FP41724@glaxowellcome.com.

[1] Abbreviations: MOPS, 3-(*N*-morpholino)propanesulfonic acid; SDS, sodium dodecyl sulfate; NA, nucleic acid; E, helicase; E·ATP, complex between E and ATP; E·NA, complex between E and NA; and E·ATP·NA, ternary complex among helicase, NA, and ATP; F, C_6-fluorescein; HF, C_6-hexachlorofluorescein; F21, 5′-GAG TCA CGA CGT TGT AAA AAA-F; HF31, HF-TTT TTT ACA ACG TCG TGA CTC TCT CTC TCT C-3′; D21, F21 without the 3′-F attached; D31, HF31 without the 5′-HF; HF16, HF-TTT TTT ACA ACG TCG-3′; D16, HF16 without the 5′-HF; OligoA, 5′-GGC GGA TCC CTG GTG CCA CGC GGT TCC CCG GTC TTT ACG GAC-3′; OligoB, 5′-GGA TCA AGC TTA CGT GAC GAC CTC CAG GTC GGC-3′; OligoC, 5′-CAC GGT GTC GAC CCT AAC ATC AGA TC-3′; OligoD, 5′-GCG TGA GCT CGT AAA AAG CGC AAC CCG CG-3′; OligoE, 5′-GCG TGA GCT CGT ACG CAG CGC AAC CCG CG-3′; OligoF, 5′-GGG ACA TGT GCA ACC CAG ACG GTC GAT TTC-3′; OligoG, 5′-GGG ACA TGT TCT TTC CTG CGT TAT CCC CTG-3′.

[2] The strand-separating activity and the processivity of hE(W501F) were inhibited at 2 mM ATP. ATP was an uncompetitive inhibitor, with an apparent K_i of 1 mM.

10.1021/bi9923860 CCC: $19.00
Published on Web 04/07/2000

Pre-steady-state and steady-state kinetic analysis of the helicase reaction indicate that the HCV helicase domain is a moderately processive enzyme ($P = 0.93$) that efficiently and *catalytically* separates dsNA at a rate of 20 bp s^{-1}, with a step size of at most 1−2 bp. The HCV helicase preferentially binds to substrates with a 3′-single-stranded tail and separates dsNA with 3′−5′ polarity (*13*). Release of the template strand is the rate-limiting step in the helicase reaction (*16*). The amino acid residues that contribute to the net movement of protein and NA, and constitute the stepping "motor", have not yet been biochemically defined.

Recently, several groups have reported structures of the HCV helicase domain in the absence or presence of bound NA (*2*−*4*). All three structures were obtained in the absence of Mg^{2+} and ATP; thus, the relationship between the observed biochemistry of the enzyme and the structure is unknown. The E·dU_8 complex crystallizes as a monomer, and differs from the apoenzyme in that three cysteinyl residues (C279, C431, and C499) are covalently modified by β-mercaptoethanol, presumably during the crystallization process (*2*, *17*).

During evolution, the HCV helicase domain has undergone subdomain duplication, creating a NA binding pocket that is comprised of two distinct but related halves. The E·NA phosphate backbone contacts are duplicated, and are structurally equivalent between the two subdomains. Two key hydrophobic interactions occur between dU_8 bases and residues W501 and V432. A model predicting that W501 and V432 contribute to the net movement of protein on NA has been proposed (*2*). Mutagenesis studies have been carried out on these and other residues in an attempt to biochemically validate the E·dU_8 structure (*17*).

We have extended our understanding of the mechanism of strand separation by analyzing the helicase activity with mutant enzymes. Data presented herein are consistent with W501 and V432 playing passive and active roles, respectively, in the helicase reaction. We also show that covalent modification of three cysteinyl residues occurs during the storage of E in buffer containing β-mercaptoethanol. The covalent modification of C279, C431, and C499 during crystallization is presumably a reflection of the reactivity of these residues in vitro.

EXPERIMENTAL PROCEDURES

Materials. Rabbit muscle pyruvate kinase, rabbit muscle lactate dehydrogenase, NADH, phosphoenolpyruvate, MOPS, ammonium sulfate, and poly[r(U)] were from Sigma Chemical Co. ATP, poly[r(C)], HisTrap affinity, HiTrap Q Sepharose, and HiTrap desalting resins were from Amersham Pharmacia Biotech. All oligomers with defined sequences were from Oligo Therapeutics, Inc. The oligomers were purified by electrophoresis on a 20% polyacrylamide gel in 6 M urea, and were quantified using the extinction coefficients provided by the manufacturer. The standard buffer was 0.05 M MOPS (K^+) and 3.5 mM $MgCl_2$ at pH 7.0.

Cloning and Expression of Helicase Mutants. HCV helicase expression constructs were based on the design of Yao et al. (*4*). The polymerase chain reaction (PCR) was used to prepare a cDNA fragment containing amino acids 1207−1657 of the HCV 1b polyprotein (*14*, *18*). OligoA was used as the 5′-primer, and oligoB was used as the 3′-primer. Vent DNA polymerase (New England Biolabs) was used to generate a blunt-ended product, which was ligated into an *Sma*I-linearized vector (pNEB193, New England Biolabs). The complete DNA sequence of the insert (pNEB193HCV1b) was determined. The appropriate DNA fragment was directionally subcloned into vector pQE9 (Qiagen) to create pQEHCV1b. The cloning of HCV helicase cDNA into vector pQE9 fused six histidinyl residues and a thrombin cleavage site to the N-terminus of the HCV helicase domain. The N-terminus of hE(wt) was MRGSHHHHH-HGSLVPRGS[1207]. The sequence of pQEHCV1b was confirmed by restriction enzyme analysis and DNA sequencing across the ligation junctions.

All three HCV 1b mutations were made using a PCR mutagenesis protocol (*19*). Following PCR mutagenesis, the products were digested with the appropriate restriction enzymes, and the mutated fragment was ligated into pNEB193HCV1b, in a three-fragment DNA ligation. OligoC was used with oligoD and oligoE to create hE(W501F) and hE(W501A), respectively. OligoF and oligoG were used to construct the hE(V432A) mutant. The entire sequence of each mutated pNEB193 construct was confirmed, and the mutated DNA fragment was directionally subcloned in pQE9 using the same methods described for the construction of hE(wt).

For protein expression, pQEHCV1b was transformed into the M15 [pREP4] expression strain and inoculated into Luria broth containing 100 μg/mL ampicillin and 25 μg/mL kanamycin. Inoculated cultures were grown to initial A_{600} of ≅0.1. An aliquot of the inoculated culture was used to seed a 1 L culture. Cultures (1 L) were grown in a 37 °C shaker until A_{600} reached ≅0.5, and then were induced with 1 mM IPTG. Induced cultures were grown at ∼22 °C overnight. Protein expression was analyzed by SDS−PAGE and Western blotting. The primary antibody used for Western blots was penta-His mouse monoclonal IgG (Qiagen).

Purification of Proteins. Cell pellets from 1 L of culture were resuspended in 10 mL of standard buffer and were pulsed three times (10 s at maximum power), with a VibraCell instrument (Sonics & Materials Inc., Danbury, CT). Sonicated extracts were sedimented at 12000*g* for 10 min at 4 °C. The pelleted fraction was discarded. The supernatant was concentrated by ammonium sulfate precipitation as described previously (*14*). Precipitated protein was resuspended in 20 mM Na^+ phosphate (pH 7.5), 10 mM imidazole, and 3.5 mM $MgCl_2$ (buffer A) and clarified by centrifugation as described above. Soluble protein was absorbed onto HisTrap resin using a peristaltic pump and a flow rate of 1 mL/min. After the resin had been washed with 10 mL of load buffer, the resin was washed with 5 mL of buffer A containing 50 mM imidazole. ATPase activity was eluted from the resin with 3 mL of buffer A containing 300 mM imidazole. Eluted protein was diluted 10-fold with 50 mM Tricine (pH 8.3), 50 mM NaCl, and 3.5 mM $MgCl_2$ (buffer B) and absorbed onto HiTrap Q resin. After being washed with 10 mL of buffer B, protein was eluted with buffer B containing 250 mM NaCl. Eluted protein was desalted using HiTrap desalting resin equilibrated in standard buffer containing 25 mM NaCl. Quality was assayed by Colloidal Blue staining of a 10% SDS−PAGE gel, and the active site concentration was estimated by titration with F21. Desalted protein could be stored frozen at −20 °C for several months without loss of activity. For mass spectrometry

experiments, hE(wt) was stored frozen at −20 °C in standard buffer containing 10 mM β-mercaptoethanol. HCV helicase lacking a histidine tag [E(wt)] was purified as described previously (*20*).

Titration of HCV Helicase with NA. Titration of helicase (E) by oligomeric nucleic acids (NA) was monitored by quenching of the intrinsic protein fluorescence upon formation of the enzyme·nucleic acid complex (E·NA) as described previously (*14*). The fractional fluorescence [$F([NA_t])$] remaining was related to the total concentration of added nucleic acid ([NA_t]) by eq 1

$$F([NA_t]) = 1 - \Delta F_\infty \frac{[E\cdot NA]}{[E_t]} \quad (1)$$

in which ΔF_∞ is the fractional fluorescence decrease resulting from conversion of E to E·NA. Because the concentration of enzyme was in many cases comparable to the dissociation constant, the concentration of E·NA for the simple scheme of eq 2a was related to [NA_t] by eq 2b. K_d is the dissociation constant of E for NA, and [E_t] is the concentration of NA binding sites.

$$E + NA \overset{K_d}{\rightleftharpoons} E\cdot NA \quad (2a)$$

$$[E\cdot NA] = \frac{[NA] + [E_t] + K_d}{2} - \frac{1}{2}\sqrt{([NA] + [E_t] + K_d)^2 - 4[E_t][NA]} \quad (2b)$$

The concentration of oligomers was calculated from the molar extinction coefficient provided by Oligo Therapeutics.

Analysis of Reaction Time Courses. The time courses for fluorescence changes were described by exponential functions (eq 3)

$$F(t) = F_0 + \sum_{i=1}^{2} F_i e^{-k_{obs,i}t} \quad (3)$$

where $F(t)$ is the observed signal at time t, F_i is the respective amplitude of the phase associated with $k_{obs,i}$, and F_0 is the final fluorescence. Linear time courses were fitted with eq 4

$$F(t) = v_o t + F_i \quad (4)$$

where $F(t)$ is the observed signal at time t, v_o is the rate of change in F_{obs} per unit time, and F_i is the initial fluorescence.

Kinetic Analysis of Helicase Activity. The time course for the formation of F21 from F21:HF31 (with [E·ATP] ≫ [F21:HF31]) was a first-order process (k_{obs}). In a simplified scheme describing the overall reaction, E·ATP binds F21:HF31 reversibly (k_{-1} and k_1). E·ATP·F21:HF31 is converted in a multiple-step reaction, with the hydrolysis of ATP, to E·ATP·HF31. This process is described by k_{eff}. Finally, E·ATP·HF31 dissociates to yield E·ATP (k_3). The first-order rate constant for the formation of F21 is related to the parameters of Scheme 1 by eq 5.

$$k_{obs} = \frac{k_{eff}[E\cdot ATP]}{[E\cdot ATP] + \frac{k_{eff} + k_{-1}}{k_1}} \quad (5)$$

Scheme 1

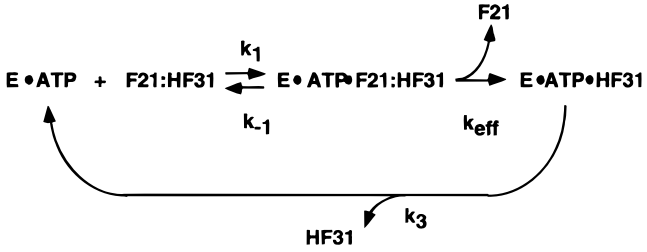

The fractional term in the denominator is equal to K_{NA}, a measurement of the affinity of E·ATP for F21:HF31. The rate of binding of ATP to E and the rate of release of ADP from E are not kinetically limiting under the experimental conditions described by Scheme 1. Because [ATP] ≫ [ADP], E is considered to be in the E·ATP form for simplicity. The k_{cat} for multiple-turnover steady-state helicase activity was calculated from the empirically determined parameters k_{eff} and k_3 using eq 6.

$$k_{cat} = \frac{k_{eff}k_3}{k_{eff} + k_3} \quad (6)$$

Processivity (P) was determined as described previously (*16*) using the empirically determined parameter, fractional strand separation. A duplex length of 21 bp (n) and a step size of 2 (m) were assumed for strand separation of F21:HF31 by helicase. Relationships between the parameters are described by eqs 7 and 8.

$$P = \frac{k_f}{k_f + k_{-1}} \quad (7)$$

$$\text{fractional strand separation} = \left(\frac{k_f}{k_f + k_{-1}}\right)^{n/m} \quad (8)$$

where k_f is the forward rate constant for each step (m) of a 2 bp separation reaction and k_{-1} is the dissociation rate constant for dissociation of E·ATP from E·ATP·F21:HF31. The dissociation rate constant for dissociation of E·ATP from E·ATP·D31 was used as a surrogate measure of k_{-1} from E·ATP·F21:HF31.

Assay of ATPase Activity. The ATPase activity associated with E was monitored by the ADP-dependent oxidation of NADH in the lactate dehydrogenase- and pyruvate kinase-coupled reaction as described previously (*14*). ATPase activity was stimulated by NA from a basal rate (v_0) to a final rate (v_∞). Equation 9 was fitted to these data

$$v(x) = \frac{(v_\infty - v_0)[x]}{K + [x]} + v_0 \quad (9)$$

where v_∞ is the maximal rate of the reaction and K is the value of [x] ([x] = [NA] or [ATP]) at the midpoint of the titration (K_{NA} or K_{ATP}).

Electrospray Ionization Mass Spectrometry. The intact mass of hE(wt) was determined using mass spectrometry. hE(wt) was desalted with a 250 μM inside diameter × 15 cm POROS R2/H column (Perceptive Biosystems, Framingham, MA). Mobile phases were (A) water with 0.05% trifluoroacetic acid and (B) 90% aqueous acetonitrile with 0.035% trifluoroacetic acid. The protein was eluted using a

gradient of 15% to 65% B. The mobile phase was coupled to a SCIEX API I mass spectrometer (PE Sciex, Concord, ON) equipped with an electrospray ionization device. Spectra were recorded in the positive ion mode. For the guanidine denaturation experiments, 100−200 pmol of protein was denatured in 4 M guanidine·HCl containing 25 mM dithiothreitol and heated at 37 °C for 20 min prior to injection onto the HPLC column.

General Methods. dsNA was made by heating a solution of stoichiometric concentrations of ssNA to 90 °C for 3 min and subsequently cooling to room temperature over the course of several hours. Fluorescence spectra were recorded on a Perkin-Elmer LS50B spectrofluorometer. Intrinsic protein fluorescence data (λ_{ex} = 290 nm and λ_{em} = 340 nm) were corrected for filter effects. F21 fluorescence was monitored with λ_{ex} = 490 nm and λ_{em} = 515 nm; HF31 fluorescence was monitored with λ_{ex} = 540 nm and λ_{em} = 560 nm with a 2.5 mm slit. Absorbance and conventional kinetic data were obtained from a Perkin-Elmer Lambda UV6 spectrophotometer. Rapid reactions were monitored on an Applied Photophysics SX.17MV spectrophotometer (Leatherhead, England). Entrance and exit slits were 2 mm in the fluorescence mode. The fluorescence of HF31 was monitored on the stopped-flow spectrofluorometer with λ_{ex} = 490 nm and λ_{em} > 520 nm. Time courses from the stopped-flow spectrofluorometer were an average of four to six experiments. Unless otherwise noted, all concentrations for stopped-flow experiments were final concentrations after mixing of reagents. Equations 1−5 and 9 were fitted to the data by a nonlinear least-squares method using SigmaPlot from Jandel Scientific (Corte Madera, CA).

RESULTS

Effect of Mutations in E on NA Binding. The structure of HCV helicase bound to dU_8 (crystallized in the absence of Mg^{2+} and an ATP analogue) suggested that W501 and V432 interacted with two uridine bases of dU_8 (*2*). We were interested in the contributions of these hydrophobic groups to the binding of E to NA and in the effects of these mutations on catalytic activity. In the simple model of Kim et al. (*2*), the energy of binding of ATP causes movement of subdomains 1A and 1B relative to subdomain 2A, resulting in a loss of contact between W501 and an oligonucleotide base. W501 reestablishes contact with an oligonucleotide base prior to hydrolysis of the bound ATP. Upon ATP hydrolysis, V432 loses contact with a bound oligonucleotide base and subdomain 2A "steps" forward at most one to two bases (Figure 1). Net movement of the helicase on the NA is achieved by hydrolysis of one ATP per "step".

The dissociation constants (K_d) for binding of helicase to NA were calculated from titration data in which the binding of NA to the enzyme was followed by monitoring the quenching of intrinsic protein fluorescence (Figure 2), or by monitoring quenching of HF-labeled oligonucleotides, as described in Experimental Procedures. Equations 1 and 2b were fitted to these data to give values for K_d and ΔF_∞. Results of these titrations are summarized in Table 1. hE(W501F) and hE(W501A) had lower affinities for NA than hE(wt). In contrast, hE(V432A) had an affinity for NA similar to that of hE(wt). The free energies of complex

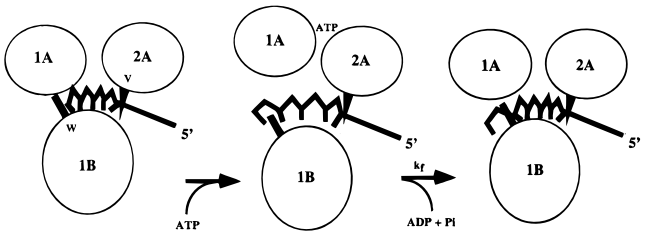

FIGURE 1: Single-stroke model for the mechanism of helicase-mediated strand separation. The structure-based model of Kim et al. (*2*) is shown. W501 (W, black box) and V432 (V, black triangle) trap five oligonucleotide bases between subdomains 1A and 2A. For clarity, only the template strand and the oligonucleotide bases in the NA-binding pocket are shown. The subdomain nomenclature of ref *27* is used for comparison with PcrA. Upon binding of ATP, relative movement of subdomains 1A and 1B causes W501 to transiently release the bound oligonucleotide. Upon hydrolysis of ATP, subdomain 2A "steps" forward and then rebinds, trapping five oligonucleotides, resulting in a net movement of one base per cycle.

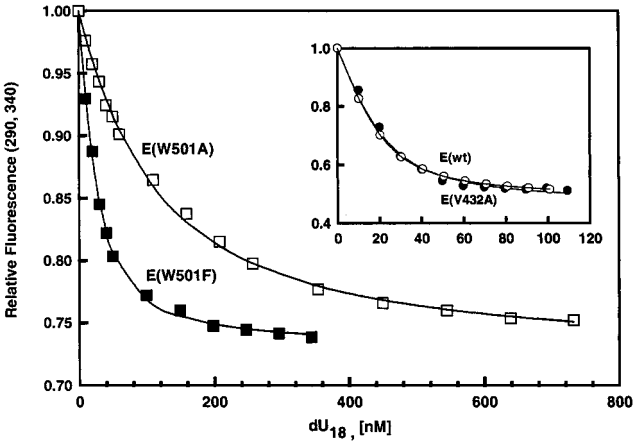

FIGURE 2: Quenching of intrinsic protein fluorescence of E upon binding of dU_{18}. The relative fluorescence (λ_{ex} = 290 nm, λ_{em} = 340 nm) of HCV helicase was measured in standard buffer after addition of dU_{18} at selected concentrations. The main panel includes titration of 22 nM hE(W501F) (■) and 44 nM hE(W501A) (□) with dU_{18}. The inset includes titration of 22 nM hE(V432A) (●) and 22 nM hE(wt) (○) with dU_{18}. Equations 1 and 2b were fitted to these data to generate the solid lines and the values listed in Table 1.

formation in kilocalories per mole at 25 °C (ΔG_f) were calculated from the measured dissociation constant (K_d) using eq 10.

$$\Delta G_f = RT \ln(K_d) \quad (10)$$

The values of ΔG_f for hE(wt), hE(W501F), and hE(W501A) binding dU_{18} were −11.2, −10.7, and −9.64 kcal/mol, respectively. Thus, the replacement of the conserved tryptophanyl residue with alaninyl resulted in the loss of 1.6 kcal/mol of binding energy.

The intrinsic tryptophan fluorescence of hE(wt) and hE(V432A) was quenched 52% by dU_{18}. In contrast, the fluorescence of hE(W501F) and hE(W501A) was only quenched 27% by dU_{18} (Figure 2). It is not obvious, from a structural comparison of the E·dU_8 complex with free E, which of the other three tryptophanyl residues of E (W532, W578, and W582) are directly involved in the quenching of hE(wt) fluorescence by dU_{18}. The three remaining tryptophanyl residues are located within subdomain 1B. W578 and

Table 1: Dissociation Constants (K_d) of HCV Helicase for Selected Oligonucleotides

oligonucleotide	protein	K_d (nM)	ΔF_∞
dU_{18}[a]	hE(wt)	6.4 ± 0.9	0.53 ± 0.01
	hE(W501F)	14.0 ± 0.6	0.27 ± 0.01
	hE(W501A)	85 ± 4	0.28 ± 0.01
	E(V423A)	6.6 ± 0.7	0.52 ± 0.01
D21[a]	hE(wt)	0.5 ± 0.1	0.43 ± 0.01
	hE(W501F)	5.2 ± 0.8	0.26 ± 0.01
	hE(W501A)	26 ± 1	0.27 ± 0.01
	hE(V432A)	0.4 ± 0.1	0.42 ± 0.01
HF16[b]	hE(wt)	1.8 ± 0.2	0.42 ± 0.01
	hE(W501F)	5 ± 1	0.38 ± 0.02
	hE(W501A)	3 ± 1	0.19 ± 0.01
	hE(V432A)	2.9 ± 0.5	0.59 ± 0.02

[a] Titration of the enzyme by oligonucleotide was monitored by the quenching of intrinsic protein fluorescence (λ_{ex} = 290 nm and λ_{em} = 340 nm). The standard buffer is defined in Experimental Procedures along with K_d and ΔF_∞. [b] Titration of HF16 with helicase was monitored with λ_{ex} = 540 nm and λ_{em} = 560 nm.

W582 are located in a 40-amino acid segment of subdomain 1B that lacks secondary structure (*2*). The fluorescence of W578 and W582 may be quenched by subtle conformational changes that occur upon binding of NA.

The hexachlorofluoresceinyl moiety on the 5′-end of HF16 contributed a small amount of binding energy to the E·NA interaction [K_d of hE(wt) for D16 was 7 nM vs 1.6 nM for HF16]. hE(wt), hE(W501F), and hE(W501A) bound HF16 with similar affinities, but the quenching of HF16 fluorescence by hE(W501A) was approximately half of that observed with hE(W501F) and hE(wt). These results suggested that the oligonucleotide was bound in slightly different environments (Table 1). In contrast, hE(V432A) quenched HF16 fluorescence more effectively than hE(wt) (Table 1), which was in agreement with the relative orientation of protein and nucleic acid, in the E·dU_8 complex (Figure 1).

NA Dissociates Slowly from E·NA and E·ATP·NA The rate constant for dissociation of NA from E·NA and E·ATP·NA was determined in the presence of a trapping agent as described by eq 11.

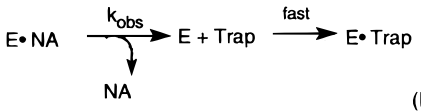

(E = E or E•ATP) (11)

The reaction was monitored on the stopped-flow spectrofluorometer by observing changes in intrinsic protein fluorescence (λ_{ex} = 290 nm, λ_{em} > 305 nm) or by the changes in fluorescence of the tagged NA (λ_{ex} = 490 nm, λ_{em} > 520 nm) associated with formation of enzyme-free NA. Several trapping agents were used to demonstrate that the value of k_{obs} was independent of the chemical properties of the trap. Furthermore, the concentration of the trapping agent in these experiments was verified to be sufficiently large that the value of k_{obs} was independent of the trap concentration. In the absence of ATP, the reaction was monophasic. In the presence of 2.0 mM ATP (K_m for ATP of 360 μM), the reaction with HF-tagged oligonucleotides was biphasic (*20*). The observed rate constants for the late phase of the reaction with ATP are reported in Table 2. The results summarized in Table 2 demonstrated that (1) the addition of a HF fluorophore to the NA decreased the value of k_{obs} significantly which suggested that the HF fluorophore interacted with the enzyme, (2) the values of k_{obs} were relatively insensitive to the trapping agent which suggested that the trapping agents were not modifying k_{obs} by forming ternary complexes with E·NA, and (3) the value of k_{obs} for dissociation of E·HF31 (0.092−0.12 s^{-1}) was similar to the value of k_{cat} for unwinding F21:HF31 (*16*).

Table 2: Rate Constants for Dissociation of E·NA Complexes[a]

NA		k_{obs} (s^{-1})	trap
D21	without ATP	0.12 ± 0.01	dextran sulfate
	with ATP	0.72 ± 0.01	dextran sulfate
D31	without ATP	0.15 ± 0.01	dextran sulfate
	with ATP	0.44 ± 0.01	dextran sulfate
F21	without ATP	0.047 ± 0.001	poly[r(U)]
	with ATP	2.19 ± 0.03	poly[r(U)]
	without ATP	0.048 ± 0.001	dextran sulfate
	with ATP	1.96 ± 0.02	dextran sulfate
HF31	without ATP	0.006 ± 0.001	dextran sulfate
	with ATP	0.12 ± 0.01[b]	dextran sulfate
	without ATP	0.007 ± 0.001	poly[r(U)]
	with ATP	0.092 ± 0.003[b]	poly[r(U)]

[a] Free helicase formed upon dissociation of the helicase·oligonucleotide complex was trapped with the indicated trapping agent (500 μM) as described in Experimental Procedures. [b] The reported rate constants were for the late phase in the biphasic process (*20*).

Table 3: Stimulation of ATPase Activity of HCV Helicase by Selected Oligonucleotides[a]

oligonucleotide	protein[b]	K_{NA} (μM)[c]	$v_\infty/[E_t]$ (s^{-1})	K_{ATP} (μM)
poly[r(U)][c]	hE(wt)	8.0 ± 2.0	43 ± 1	150 ± 20
	hE(W501F)	24 ± 6	43 ± 2	190 ± 30
	hE(W501A)	180 ± 20	26 ± 1	170 ± 20
	hE(V432A)	49 ± 9	58 ± 3	190 ± 30
poly[r(C)][c]	hE(wt)	30 ± 7	17 ± 1	
	hE(W501F)	500 ± 100	20 ± 1	
	hE(W501A)	4600 ± 1000	17 ± 2	
	hE(V432A)	500 ± 100	12 ± 1	

[a] ATPase assays in standard buffer were initiated with enzyme at 25 °C as described in Experimental Procedures. [b] E(W501F), hE(W501A), and hE(V432A) active site concentrations were determined by titration with F21. K_{NA} values were determined by fitting eq 9 to the data. [c] Base concentrations of poly[r(U)] and poly[r(C)] were determined spectrophotometrically with an ϵ_{260} of 9.35 mM^{-1} cm^{-1} and an ϵ_{269} of 6.2 mM^{-1} cm^{-1}.

Effect of Mutations on the Interaction of E·ATP with NA. An indirect measure of the affinity of NA for the E·ATP complex can be estimated for the value of K_{NA} in the oligonucleotide-stimulated ATPase reaction. hE(W501F)·ATP, hE(W501A)·ATP, and hE(V432A)·ATP had lower affinities for poly[r(U)] than hE(wt)·ATP (Table 3). The calculated ΔG_f values for E·ATP binding poly[r(U)] were −6.95, −6.3, −5.87, and −5.09 kcal/mol for hE(wt), hE(W501F), hE(V432A), and hE(W501A), respectively. The W501A mutation resulted in the loss of less than 2 kcal/mol of binding energy for formation of E·ATP·poly[r(U)].

Poly[r(C)] was less efficient as an ATPase effector than poly[r(U)]. Both the affinity of E for poly[r(C)] and the value of k_{cat} with poly[r(C)] as the NA effector were lower than the values with poly[r(U)] as the NA effector. The W501A mutation resulted in a loss of approximately 2.3 kcal/mol, and the W501F and V432A mutations resulted in a loss of approximately 1 kcal/mol for the formation of E·ATP·poly[r(C)].

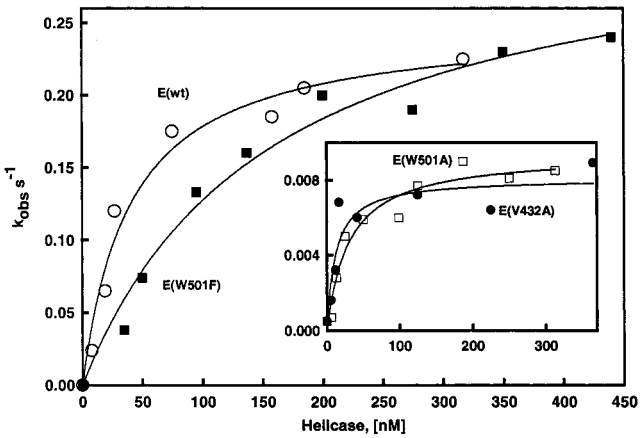

FIGURE 3: Strand separation of F21:HF31 by HCV helicase and ATP. The value of the first-order rate constant for strand separation (k_{obs}) of 15 nM F21:HF31 (λ_{ex} = 490 nm, λ_{em} = 515 nm) was determined at various enzyme concentrations with hE(wt) (○), hE(V432A) (●), hE(W501A) (□), and hE(W501F) (■). Each reaction was initiated with ATP. Values of k_{eff} and K_{NA} for the strand separation reaction were estimated from these data using eq 5 (Table 4).

The catalytic efficiency of the enzyme as an ATPase was not dramatically affected by mutagenesis of W501 or V432 (Table 3). K_{ATP} values did not differ significantly among the four proteins that were tested, whereas the values of k_{cat} were within a 2-fold range. Similarly, the k_{cat}/K_m values ranged from 0.306 μM^{-1} s^{-1} for hE(V423A) to 0.157 μM^{-1} s^{-1} for hE(W501A). These differences were not considered to be experimentally significant.

Effect of Mutations in E on Strand-Separating Activity. Helicase activity is typically analyzed by native gel electrophoresis of the single-stranded products. This method has limitations for studying the mechanism of strand separation. Recently, several fluorescence-based assays have been developed for the study of helicases (*21*, *22*). We chose to use the fluorescence resonance energy assay developed by Bjornson et al. for mechanistic studies of *Escherichia coli* Rep helicase (*21*). The substrate for this assay is a NA duplex of fluorescein- and hexachlorofluorescein-tagged oligomers. The fluorescence of the fluoresceinyl tag (λ_{ex} = 490 nm, λ_{em} = 515 nm) in the duplex structure is proposed to be quenched by fluorescence resonance energy transfer to the hexachlorofluoresceinyl tag. Consequently, enzymatic separation of the fluoresceinyl and hexachlorofluoresceinyl tags resulted in an increase in the fluorescence signal of the fluorescein tag. The fluorescence of F21 was 9-fold greater than that of F21:HF31 and approximately 2-fold greater than that observed by Bjornson et al. with an analogously tagged duplex NA (*16*, *21*).

Because the affinity of hE(W501F)·ATP for F21:HF31 was lower than that of hE(wt)·ATP for F21:HF31 (see below) and the catalytic activities of hE(W501A) and hE(V432A) were greatly reduced relative to that of hE(wt), it was not possible to accurately measure the effect of the mutations on k_{cat} or K_{NA} by steady-state turnover experiments. We estimated these parameters by monitoring reactions under conditions where [E] ≫ [F21:HF31] and [ATP] ≫ K_{ATP} (Figure 3 and Table 4). The strand separation experiments monitor F21 formation and not the rate-limiting dissociation of E·HF31 (k_3 in Scheme 1). The dependence of k_{obs} on [E] is given by eq 5. From the dependence of k_{obs} on [E], the value of k_{eff} for strand separation was estimated (Table 4). With this value for k_{eff} and the value of k_3 (Table 4), the value of k_{cat} was calculated by eq 6. The measured k_{eff} values of hE(W501F), hE(W501A), and hE(V432A) were 136%, 3.8%, and 3.2% of that of hE(wt). The calculated k_{cat} values of hE(W501F), hE(W501A), and hE(V432A) were 227%, 14%, and 11% of that of hE(wt) (Table 4). In summary, hE(W501F) had greater strand-separating activity and calculated steady-state activity, whereas both hE(W501A) and hE(V432A) had greatly reduced strand-separating and calculated steady-state activity.

Table 4: Strand-Separating Activity of hE(wt) and Mutant Enzymes

protein	K_{NA}[a] (nM)	k_{eff} (s^{-1})	k_3 (s^{-1})	calculated k_{cat}[b] (s^{-1})
hE(wt)	40 ± 9	0.25 ± 0.02	0.092 ± 0.003	0.066
hE(W501F)	170 ± 40	0.34 ± 0.03	0.264 ± 0.003	0.15
hE(W501A)	31 ± 9	0.0095 ± 0.0007	1.074 ± 0.005	0.0094
hE(V432A)	11 ± 6	0.0082 ± 0.0008	0.086 ± 0.006	0.0075

[a] K_{NA} and k_{eff} were estimated by fitting eq 5 to the data presented in Figure 3B. [b] The calculated k_{cat} value for the steady-state helicase reaction was estimated using eq 6.

Table 5: Processivity and Calculated k_f Values of HCV Helicase Mutants

protein	k_{-1} (s^{-1})[a]	processivity	calculated k_f (s^{-1})
hE(wt)	0.44 ± 0.01	0.93	5.9
hE(W501F)	1.02 ± 0.02	0.89	8.3
hE(W501A)	4.3 ± 0.1	≤0.66[b]	8.3
hE(V432A)	0.37 ± 0.01	≤0.66	0.72

[a] D31 release (k_{-1}) was initiated by the simultaneous addition of 1 mM ATP with 500 μM dextran sulfate in standard buffer at 25 °C to E·D31. Values for k_{-1} were estimated by fitting eq 3 to the data. [b] Maximal values for the processivity of hE(W501A) and hE(V432A) were estimated assuming the minimal detectable fractional strand separation value of 0.01, and a step size of 2.

The processivity of E is related to rate constants k_{-1} and k_f by eq 7. The value of k_{-1} was empirically determined for a surrogate model, whereas the value of k_f was estimated using the value of k_{-1}, the fractional strand separation value, and the step size of E (parameter *m* of eq 8), which was estimated to be 2 bp (*16*). Direct determination of the value of k_{-1} for dissociation E·ATP from E·ATP·F21:HF31 was complicated by the partitioning between F21 formation and the dissociation of F21:HF31. Consequently, the rate constants for dissociation of E·ATP from hE(wt)·ATP·D31 and hE(W501F)·ATP·D31 were used as a surrogate model to estimate k_{-1}. The values of the dissociation rate constants were 0.44 ± 0.01 and 1.02 ± 0.02 s^{-1} for hE(wt) and hE(W501F), respectively (Table 5). These results were consistent with the observed NA binding affinity of hE(wt) and hE(W501F) (Tables 1 and 3), and the reduced processivity of hE(W501F).

The fractional strand separation (eq 8) and the dissociation rate constant (k_{-1}) were determined in the presence of ATP and a trap for hE(wt) and hE(W501F) (Figure 4 and Table 5). The fractional strand separation of hE(W501F)·F21:HF31 was 0.28. This corresponded to a processivity of 0.89 (calculated using eqs 7 and 8). The corresponding values for hE(wt) were 0.44 and 0.93, respectively (*16*). The lag phase of the strand separation reaction of F21:HF31 by hE(W501F) (Figure 4B, inset) was identical to that observed

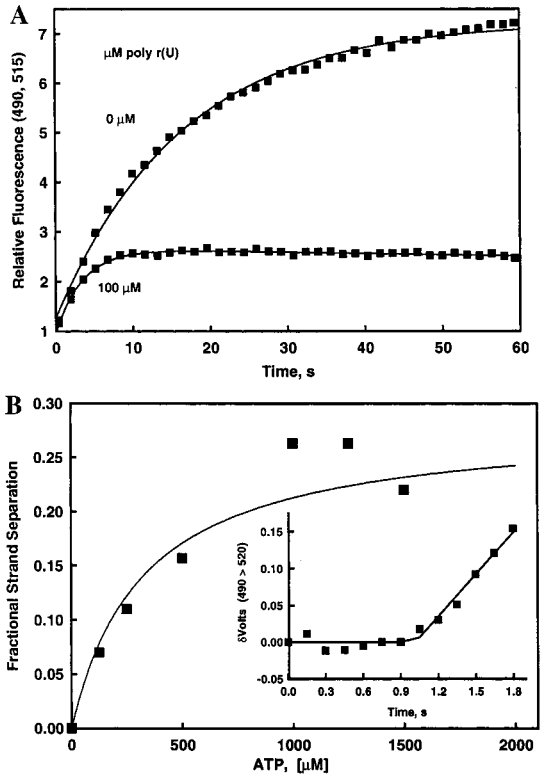

FIGURE 4: Processivity of hE(W501F). (A) The relative fluorescence of 50 nM enzyme and 25 nM F21:HF31 in the standard buffer at 25 °C was monitored with $\lambda_{ex} = 490$ nm and $\lambda_{em} = 515$ nm. Reactions were initiated with 1 mM ATP in the presence or absence of 100 μM poly[r(U)]. Equation 3 was fitted to the data, and the best fits are shown. The K_d of hE(W501F) for F21:HF31 in the absence of ATP was 3 ± 1 nM. (B) Fractional strand separation of F21:HF31 by hE(W501F). The maximal extent of strand separation was dependent on ATP concentration. The maximal value for fractional strand separation [in the presence of ATP and 100 μM poly[r(U)]] was 0.28, and the concentration of ATP yielding 50% of this value was 330 μM. The inset shows the time course for the reaction of hE(W501F)·F21:HF31 with ATP in the absence of the competitor poly[r(U)]. hE(W501F) (440 nM) and F21:HF31 (15 nM) reacted with 1 mM ATP. The extent of formation of F21 was measured with the stopped-flow spectrofluorometer. The full response range of the instrument was 4 V. The length of the lag phase was 1.02 ± 0.03 s, which was consistent with a step size of at most 2 bp.

with E(wt) (*16*), consistent with a step size of at most 2 bp (*16*). The forward rate constant for strand separation (k_f) was estimated using the observed k_{-1} and processivity values for hE(wt) and hE(W501F) and eq 7. These calculated values were 5.9 and 8.3 s^{-1} for hE(wt) and hE(W501F), respectively.

In contrast to our results with hE(wt) and hE(W501F), simultaneous addition of ATP and poly[r(U)] to hE(W501A)·F21:HF31 or hE(V432A)·F21:HF31 resulted in no change of fluorescence that is attributed to the formation of F21 (data not shown). If the minimal fluorescence change that can be observed under these conditions corresponded to a fractional strand separation of 0.01, then the processivity of hE(W501A) and hE(V432A) (F21:HF31 as the substrate) was calculated from eq 8 and a step size of 2 to be equal to 0.66. An upper limit for the value of k_f could be estimated from this processivity value if the value for the dissociation constant (k_{-1}) was known. The rate of dissociation of E·ATP from E·ATP·D31 was used as a surrogate value for the dissociation of E·ATP from E·ATP·F21:HF31. These

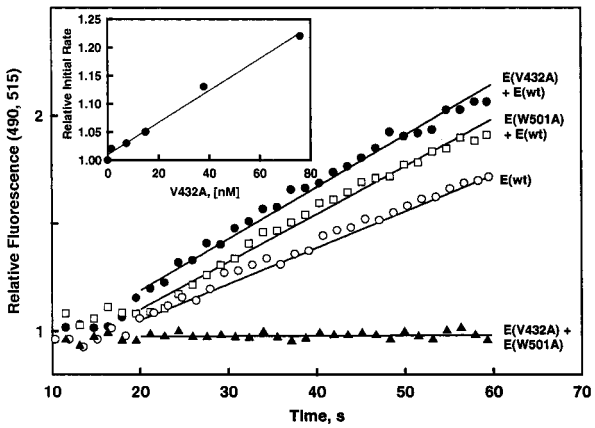

FIGURE 5: hE(W501A) and hE(V432A) were not dominant negative suppressors of hE(wt) helicase activity. The relative fluorescence ($\lambda_{ex} = 490$ nm, $\lambda_{em} = 515$ nm) of 100 nM F21:HF31 in standard buffer at 25 °C containing 2 mM ATP is shown as a function of time. Reactions were initiated at 20 s with 1.5 nM hE(wt) (○) alone, or with 1.5 nM hE(wt) in combination with 15 nM hE(V432A) (●) or 15 nM hE(W501A) (□). The lower trace was generated by initiating the reaction with 15 nM hE(V432A) and 15 nM hE(W501A) (▲). Equation 4 was fitted to the data to give the solid lines. The inset shows the dependence of the normalized rate of initial strand separation of 100 nM F21:HF31 by 8 nM hE(wt) on the concentration of hE(V432A). The observed rate of strand separation of 100 nM F21:HF31 by 8 nM hE(wt) in the absence of hE(V432A) was normalized to 1.

values were 0.37 ± 0.01 and 4.3 ± 0.1 s^{-1} for hE(V432A) and hE(W501A), respectively. Using these values and a processivity value of 0.66, eq 7 was used to calculate k_f values of 0.72 and 8.3 s^{-1} for hE(V432A) and hE(W501A), respectively (Table 5). Thus, the major effect of the V432A mutation was on the forward rate constant for strand separation (k_f), and the major effect of the W501A mutation was on the dissociation rate constant (k_{-1}).

Effect of hE(W501A) and hE(V432A) on hE(wt) Helicase Activity. Under steady-state conditions, the ATPase and helicase activities of HCV helicase are linearly dependent upon protein concentration (*14*, *16*). Biophysical analyses and the crystal structure of the E·dU_8 complex are consistent with the enzyme existing as a monomer in solution (*2*). It is possible that the enzyme could *transiently* dimerize to the catalytically active form during the enzymatic cycle at concentrations below or above the ranges tested with E(wt) (1.5−80 nM). The reduced helicase activity of hE(W501A) and hE(V432A) allowed us to test the activity of hE(wt) in the presence of varying amounts of these mutants. If transient dimerization were required for helicase activity, then dimerization of hE(wt) with hE(V432A) or hE(W501A) should measurably reduce the observed helicase activity. If the activity of hE(wt) was unaffected by dimerization with hE(V432A) or hE(W501A), then no inhibition would be observed.

When [F21:HF31] ≫ K_{NA} and [F21:HF31] ≫ [E], no inhibition of hE(wt) was observed at ratios of wild-type:mutant enzymes ranging from 1:1 to 1:10 (Figure 5). Thus, hE(V432A) and hE(W501A) did not detectably dimerize with hE(wt) under the experimental conditions used in the experiments whose results are depicted in Figure 5. The observed rate increase in the presence of increasing amounts of hE(V432A) was consistent with hE(wt) functioning as a monomeric enzyme between 1.5 and 80 nM hE(V432A).

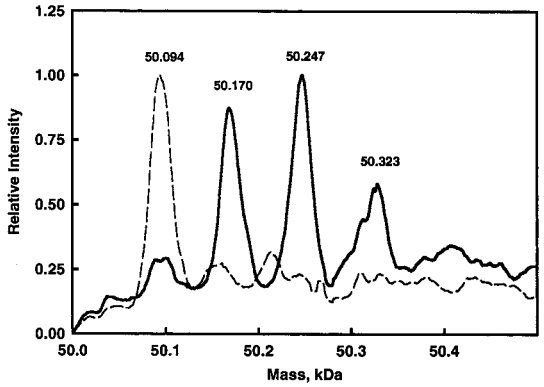

FIGURE 6: Electrospray ionization mass spectrometry of HCV helicase. hE(wt) (100 pmol) was subjected to electrospray mass ionization. The relative peak intensities of the molecular ion peaks and the absolute molecular masses (kilodaltons) are shown: 100 pmol of hE(wt) purified and stored in the presence of 10 mM β-mercaptoethanol (—) and 100 pmol of guanidine-denatured and dithiothreitol-reduced hE(wt) (- - -).

HCV Helicase Is Posttranslationally Modified in Vitro by β-Mercaptoethanol. The crystal structure of the E·dU_8 complex demonstrated that three cysteinyl residues (C279, C431, and C499) were covalently modifed by β-mercaptoethanol, presumably during the crystallization process (*17*). Our mutagenesis data indicated that mutagenesis of V432 and W501 profoundly affected helicase activity. Consequently, it was of interest to determine if the covalent modification occurred in solution. We analyzed the apparent molecular weight of hE(wt) purified in the presence or absence of β-mercaptoethanol by electrospray ionization mass spectrometry. These results are presented in Figure 6.

hE(wt) purified and stored in the presence of 10 mM β-mercaptoethanol was heterogeneous, as determined by mass spectrometry (Figure 6). The results indicated that three positions were modified by a common adduct of 73 mass units. The modification was sensitive to removal by denaturation and reduction in the presence of guanidine and dithiothreitol. These results suggested that β-mercaptoethanol formed adducts with hE(wt). hE(wt), hE(V432A), and E(wt) (*20*) were purified in the absence of β-mercaptoethanol and were analyzed as described above. No significant modification of E was observed. β-Mercaptoethanol-modified hE(wt) exhibited biphasic kinetics in strand separation assays (data not shown).

DISCUSSION

Helicases *catalyze* the ATP-dependent strand separation of dsNA. Recent mechanistic studies on *E. coli* Rep helicase are the basis for a detailed understanding of the kinetic mechanism for strand separation by a helicase (*23*, *24*). Lohman has classified the mechanism for helicase action as being either "active" or "passive" (*1*). In a passive-type mechanism, the enzyme binds preferentially to ssNA and separates dsNA by binding to ssNA that is formed transiently from the duplex as a result of thermal fluctuations. The enzyme is translocated unidirectionally by the hydrolysis of ATP. In contrast, an active mechanism requires that the enzyme bind to both dsNA and ssNA. The enzyme destabilizes multiple base pairs during each catalytic step, and the mechanism requires that the enzyme have multiple binding sites either on the same subunit or as an oligomeric protein. During catalysis fueled by ATP, one NA binding site alternatively binds dsNA and ssNA as the enzyme rolls along the dsNA. Two readily demonstrable differences between an active and a passive mechanism are as follows: (1) an active mechanism requires multiple NA binding sites on the catalyst and (2) an active mechanism separates multiple base pairs during a catalytic cycle. In the case of *E. coli* Rep helicase, NA induces dimerization of the monomeric protein to generate two NA binding sites on the catalytically active form of the enzyme (*25*).

Several RNA helicases, including p68 and RNA helicase A and vaccinia helicase NPH-II, have been suggested to be active in the monomeric form. Sequence analysis of these enzymes indicates multiple dsNA-binding domains per monomeric enzyme (*26*). However, as noted by Lohman and Bjornson, the assembly states of these proteins in the presence of substrates have not been determined (*9*). In contrast to findings with other well-studied helicases, such as *E. coli* Rep helicase (*28*), T4 helicase (*29*), and DnaB helicase (*30*), ultracentrifugation, gel filtration, chemical cross-linking, and activity measurements indicated that HCV helicase was a monomeric protein in the presence of NA and/or ATP. The crystal structure of a E·dU_8 complex also indicates a monomeric form of the enzyme (*2*). Because HCV helicase contains a single NA binding site per monomer (*14*), the active species of this enzyme had a single NA binding site.

The crystal structure for a helicase from *Bacillus stearothermophilus* (PcrA) indicated that PcrA is a monomeric protein (*27*, *31*). In an elegant study that compared crystal structures of substrate and product complexes, it is apparent that monomeric PcrA is capable of functioning as a helicase (*27*). The two crystal structures identified several changes in the structure of nucleic acid and protein that exist during the binding of a nonhydrolyzable ATP analogue (ADPNP). The energy of binding ADPNP is used to drive conformational changes both in the substrate and in the enzyme. The binding energy is also used to create a novel *transient* dsNA binding site at the interface between two protein subdomains (*27*). It is not known if a similar transient dsNA binding site is created on the surface of the HCV helicase upon binding of ATP.

Residue W259 of PcrA functions just like W501 of HCV helicase, in that it stabilizes the E·NA complex. The relative position of W259 does not change dramatically between the substrate and product complexes (*27*). In contrast to W259, the relative position of F64 of PcrA changes dramatically upon binding of ADPNP. This residue may constitute part of the stepping "motor" for PcrA helicase. It will be interesting to determine the positions of W501 and V432 in an analogous substrate and product complex with HCV helicase. It is likely that comparison of two such structures would be useful in identifying additional residues involved in strand separation of dsNA.

Data presented herein demonstrate that three cysteinyl residues on the surface of HCV helicase are intrinsically reactive with β-mercaptoethanol and, on the basis of the E·dU_8 structure, are likely to be C279, C431, and C499 (*17*). We have shown that mutagenesis of V432 and W501 can profoundly affect helicase activity; therefore, it is important to determine if C431 and C499 also contribute to the helicase mechanism. C431 is of particular interest because of the

proximity to a critical part of the forward stepping "motor" of HCV helicase (V432). Future mutagenesis studies of C431 and C499 of NS3, in a replicon-based system, will be valuable in determining the importance of these residues in the replication cycle (*32*).

Several laboratories have routinely stored helicases in the presence of 5−15 mM β-mercaptoethanol (*2*, *21*, *33*). Our laboratory analyzed a preparation of UvrD by mass spectrometry and found that 50% of the protein was modified by an adduct, consistent with it being β-mercaptoethanol. The kinetics of quenching of a HF-labeled oligonucleotide was biphasic with this preparation of UvrD.[3] We attributed the biphasic kinetics of quenching to the presence of two different forms of enzyme that differ in their kinetic properties. Data presented herein and in Kim et al. (*17*) show that the use of β-mercaptoethanol in storage buffers should be avoided for kinetic studies of helicase activity.

Data from equilibrium sedimentation velocity and size exclusion chromatography experiments indicated that C-terminal deletion mutants of UvrD helicase are monomeric under the experimental conditions that were used (*33*). UvrD is capable of separating dsNA under conditions of high E:NA ratios, but it is not known if the C-terminal deletion mutants have a dominant negative phenotype in a helicase assay with full-length UvrD. In vivo complementation experiments with mutant UvrDK35M result in a dominant negative phenotype, suggesting that when UvrD acts *stoichiometrically* as a helicase it is sensitive to inhibition by interaction with the mutant enzyme (*34*). Under steady-state turnover conditions (substrate in excess over enzyme), no dominant negative inhibition of hE(wt) was observed with hE(W501A) or hE-(V432A), confirming our empirical observations that the HCV helicase can function as a monomeric, *catalytic* helicase.

The kinetic partitioning of helicase between forward movement (k_f) and dissociation from template (k_{-1}) determines the overall processivity of the enzyme (eq 7). Herein, we have used the term "passive" to describe changes that primarily affect the dissociation rate of E from the template (k_{-1}) and the term "active" to describe changes that primarily affect the rate of the forward strand separation step (k_f). Mutagenesis of W501 primarily affected k_{-1}, suggesting that W501 played a passive role in the helicase reaction. Mutagenesis of V432 primarily affected k_f, suggesting that V432 played an active role in the helicase reaction.

The structure-based model of Kim et al. (*2*) predicts that oligonucleotide bases "slip" by W501 during the enzymatic cycle, suggesting that destabilization of the interaction between W501 and template by mutation can affect both k_f and k_{-1} simultaneously. Data presented herein are consistent with this prediction. The model predicts that the number of oligonucleotide bases between W501 and V432 should differ between substrate and product complexes. The model also predicts a defined "firing" order, with the release and rebinding of W501 to the template occurring prior to forward movement of V432. Both of these predictions can be tested if a substrate complex of HCV helicase analogous to that of PcrA can be obtained (*27*). Future experiments investigating the contribution of the bound NA to the mechanism should help clarify the details of the structure-based model of HCV helicase.

The mutations described herein are of academic and practical importance. It should be possible to test if inhibitors derive binding energy from W501 or V432, by comparing the inhibition of mutant and wild-type enzymes. Under conditions used for high throughput screening of chemical libraries, the time course for fractional product formation is described by eq 12.

$$P(t) = 1 - e^{-(k_{cat}/K_{NA})[E]t} \quad (12)$$

The kinetic parameters of E dictate that under normal assay conditions most of the enzyme is in the unbound or free form. Once E·ATP·NA is formed, E·ATP rapidly separates dsNA ($t \approx 1$ s) and the association rate constant for small molecules becomes limiting [i.e., k_1 for ATP (*14*) associating with E·NA = 0.4 μM^{-1} s^{-1}]. The short half-life of the E·ATP·NA complex and the low association rate constant for small molecules (such as ATP) reduce the probability of detecting an uncompetitive inhibitor in assays with E(wt).

Mutations that diminish the value of k_{cat} but have normal or reduced values for K_{NA} would allow assays to be run under conditions where E is in the E·ATP·NA form, facilitating the discovery of uncompetitive inhibitors. hE(V432A) would be a useful starting point toward the discovery of inhibitors that exploit a non-substrate binding region that allosterically modulates helicase activity.

ACKNOWLEDGMENT

We thank Mary H. Hanlon for bringing to our attention the observation that storage of E in the presence of β-mercaptoethanol altered the activity of E.

REFERENCES

1. Lohman, T. M. (1993) *J. Biol. Chem. 268*, 2269−2272.
2. Kim, J. L., Morgenstern, K. A., Griffith, J. P., Dwyer, M. D., Thomson, J. A., Murcko, M. A., Lin, C., and Caron, P. R. (1998) *Structure 6*, 89−100.
3. Cho, H.-S., Ha, N.-C., Kang, L.-W., Chung, K. M., Bac, S. H., Jang, S. K., and Oh, B.-H. (1998) *J. Biol. Chem. 273*, 15045−15052.
4. Yao, N., Hesson, T., Cable, M., Hong, Z., Kwong, A. D., Le, H. V., and Weber, P. C. (1997) *Nat. Struct. Biol. 4*, 463−467.
5. Yu, X., Jesewska, M. J., Bujalowski, W., and Egelman, E. H. (1996) *J. Mol. Biol. 259*, 7−14.
6. Koonin, E. V. (1992) *Trends Biochem. Sci. 17*, 495−497.
7. McSwiggen, J. A., Bear, D. G., and Von Hippel, P. H. (1988) *J. Mol. Biol. 199*, 609−606.
8. Hacker, K. J., and Johnson, K. A. (1997) *Biochemistry 36*, 14080−14087.
9. Lohman, T. M., and Bjornson, K. P. (1996) *Annu. Rev. Biochem. 65*, 169−214.
10. Blight, K. J., Kolykhalov, A. A., Reed, K. E., Agapov, E. V., and Rice, C. M. (1998) *Antiviral Ther. 3*, 83−91.
11. Kwong, A. D., Kim, J. L., Rao, G., Lipovsek, D., and Raybuck, S. A. (1998) *Antiviral Res. 40*, 1−18.
12. Suzich, J. A., Tamura, J. K., Palmer-Hill, F., Warrener, P., Grakoui, A., Rice, C. M., Feinstone, S. M., and Collett, M. S. (1993) *J. Virol. 67*, 6152−6158.
13. Kim, D. W., Gwack, Y., Han, J. H., and Choe, J. (1995) *Biochem. Biophys. Res. Commun. 215*, 160−166.
14. Preugschat, F., Averett, D. R., Clarke, B. E., and Porter, D. J. T. (1996) *J. Biol. Chem. 271*, 24449−24457.
15. Porter, D. J. T. (1998) *J. Biol. Chem. 273*, 7390−7396.

[3] David J. T. Porter and Roderick G. Davis, unpublished data.

16. Porter, D. J. T., Short, S. A., Hanlon, M. H., Preugschat, F., Wilson, J. E., Willard, D. H., Jr., and Consler, T. G. (1998) *J. Biol. Chem 273*, 18906−18914.
17. Kim, J. L., Morgenstern, K. A., Caron, P., and Lin, C. (1999) Patent Appl. WO 9909148.
18. Clarke, B. E., Brown, A. L., Grace, K. G., Hastings, G. Z., Brown, F., Rowlands, D. J., and Francis, M. J. (1990) *J. Gen. Virol. 71*, 1109−1117.
19. Fetter, J., Cohen, J., Danger, D., Sanders-Loehr, J., and Theil, E. C. (1997) *JBIC, J. Biol. Inorg. Chem. 2*, 652−651.
20. Porter, D. J. T. (1998) *J. Biol. Chem. 273*, 14247−14253.
21. Bjornson, K. P., Amaratunga, M., Moore, K. J. M., and Lohman, T. M. (1994) *Biochemistry 33*, 14306−14316.
22. Raney, K. D., Sowers, L. C., Millar, D. P., and Benkovic, S. J. (1994) *Proc. Natl. Acad. Sci. U.S.A. 91*, 6644−6648.
23. Ali, J. A., and Lohman, T. M. (1997) *Science 275*, 377−380.
24. Amaratunga, M., and Lohman, T. M. (1993) *Biochemistry 32* (27), 6815−6820.
25. Wong, I., Chao, K. L., Bujalowski, W., and Lohman, T. M. (1992) *J. Biol. Chem. 267*, 7596−7610.
26. Gibson, T. J., and Thompson, J. D. (1994) *Nucleic Acids Res. 22*, 2552−2556.
27. Velankar, S. S., Soultanos, P., Dillingham, M. S., Subramanya, H. S., and Wigley, D. B. (1999) *Cell 97*, 75−84.
28. Chao, K., and Lohman, T. M. (1991) *J. Mol. Biol. 221*, 1165−1181.
29. Dong, F., Gogol, E. P., and von Hippel, P. H. (1995) *J. Biol. Chem. 270*, 7462−7473.
30. Bujalowski, W., and Jezewska, M. J. (1995) *Biochemistry 34*, 8513−8519.
31. Bird, L. E., Brannigan, J. A., Subramanya, H. S., and Wigley, D. B. (1998) *Nucleic Acids Res. 26*, 2686−2693.
32. Lohmann, V., Korner, F., Koch, J.-O., Herian, U., Theilmann, L., and Bartenschlager, R. (1999) *Science 285*, 110−113.
33. Mechanic, L. E., Lata, M. E., and Matson, S. W. (1999) *J. Biol. Chem. 274*, 12488−12498.
34. George, J. W., Brosh, R. M., Jr., and Matson, S. W. (1994) *J. Mol. Biol. 235*, 424−435.

BI9923860